

Application of Hooke & Jeeves Algorithm in Optimizing Fusion Zone Grain Size and Hardness of Pulsed Current Micro Plasma Arc Welded AISI 304L Sheets

Kondapalli Siva Prasad^{1*}, Chalamalasetti Srinivasa Rao², Damera Nageswara Rao³

¹Department of Mechanical Engineering, Anil Neerukonda Institute of Technology & Sciences, Visakhapatnam, India

²Department of Mechanical Engineering, Andhra University, Visakhapatnam, India

³Centurion University of Technology & Management, Odisha, India

Email: *kspanits@gmail.com

Received April 2, 2012; revised May 6, 2012; accepted May 27, 2012

ABSTRACT

AISI 304L is an austenitic Chromium-Nickel stainless steel offering the optimum combination of corrosion resistance, strength and ductility. These attributes make it a favorite for many mechanical components. The paper focuses on developing mathematical models to predict grain size and hardness of pulsed current micro plasma arc welded AISI 304L joints. Four factors, five level, central composite rotatable design matrix is used to optimize the number of experiments. The mathematical models have been developed by Response Surface Method (RSM) and its adequacy is checked by Analysis of Variance (ANOVA) technique. By using the developed mathematical models, grain size and hardness of the weld joints can be predicted with 99% confidence level. The developed mathematical models have been optimized using Hooke and Jeeves algorithm to minimize grain size and maximize the hardness.

Keywords: Pulsed Current Micro Plasma Arc Welding; AISI 304L; Grain Size; Hardness; Hooke & Jeeves Algorithm

1. Introduction

In welding processes, the input parameters have greater influence on the mechanical properties of the weld joints. By varying the input process parameters, the output could be changed with significant variation in their mechanical properties. Accordingly, welding is usually selected to get a welded joint with excellent mechanical properties. To determine these welding combinations that would lead to excellent mechanical properties, different methods and approaches have been used. Various optimization methods can be applied to define the desired output variables through developing mathematical models to specify the relationship between the input parameters and output variables. One of the most widely used methods to solve this problem is Response Surface Methodology (RSM), in which the unknown mechanism with an appropriate empirical model is approximated, being the function of representing a RSM.

Welding thin sheets is quite different from welding thick sections, because during welding of thin sheets many problems are experienced. These problems are usually linked with heat input. Fusion welding generally involves joining of metals by application of heat for

melting of metals to be joined. Almost all the conventional arc welding processes offer high heat input, which in turn leads to various problems such as burn through or melt trough, distortion, porosity, buckling warping & twisting of welded sheets, grain coarsening, evaporation of useful elements present in coating of the sheets, joint gap variation during welding, fume generation from coated sheets etc. Use of proper welding process, procedure and technique is one tool to address this issue [1]. Micro Plasma arc Welding (MPAW) is a good process for joining thin sheet, but it suffers high equipment cost compared to Gas Tungsten Arc Welding (GTAW). However it is more economical when compare with Laser Beam welding and Electron Beam Welding processes.

Pulsed current MPAW involves cycling the welding current at selected regular frequency. The maximum current is selected to give adequate penetration and bead contour, while the minimum is set at a level sufficient to maintain a stable arc [2,3]. This permits arc energy to be used effectively to fuse a spot of controlled dimensions in a short time producing the weld as a series of overlapping nuggets. By contrast, in constant current welding, the heat required to melt the base material is supplied only during the peak current pulses allowing the heat to dissipate into the base material leading to narrower Heat

*Corresponding author.

Affected Zone (HAZ). Advantages include improved bead contours, greater tolerance to heat sink variations, lower heat input requirements, reduced residual stresses and distortion, refinement of fusion zone microstructure and reduced width of HAZ. There are four independent parameters that influence the process are peak current, back current, pulse rate and pulse width.

From the literature review [4-18] it is understood that in most of the works reported the effect of welding current, arc voltage, welding speed, wire feed rate, magnitude of ion gas flow, torch stand-off, plasma gas flow rate on weld quality characteristics like front melting width, back melting width, weld reinforcement, welding groove root penetration, welding groove width, front-side undercut are considered. However, much effort was not made to develop mathematical models to predict the same especially when welding thin sheets in a flat position. Hence an attempt is made to correlate important pulsed current MPAW process parameters to grain size and hardness of the weld joints by developing mathematical models by using statistical tools such as design of experiments, analysis of variance and regression analysis. The grain size and hardness of the weld joints was optimized using Hooke & Jeeves algorithm.

2. Experimental Procedure

Austenitic stainless steel (AISI 304L) sheets of 100 × 150 × 0.25 mm are welded autogenously with square butt joint without edge preparation. The chemical composition of AISI 304L stainless steel sheet is given in **Table 1**. High purity argon gas (99.99%) is used as a shielding gas and a trailing gas right after welding to prevent absorption of oxygen and nitrogen from the atmosphere. From the literature four important factors of pulsed current MPAW as presented in **Table 2** are chosen. The welding has been carried out under the welding conditions presented in **Table 3**. A large number of trail experiments were carried out using 0.25 mm thick AISI 304L sheets to find out the feasible working limits of pulsed current MPAW process parameters. Due to wide range of factors, it has been decided to use four factors, five levels, rotatable central composite design matrix to perform the number of experiments for investigation. **Table 4** indicates the 31 set of coded conditions used to form the design matrix. The first sixteen experimental conditions (rows) have been formed for main effects. The next eight experimental conditions are called as corner points and the last seven experimental conditions are known as center points.

Table 1. Chemical composition of AISI 304L (wt%).

C	Si	Mn	P	S	Cr	Ni	Mo	Ti	N
0.021	0.35	1.27	0.030	0.001	18.10	8.02	-	-	0.053

Table 2. Important factors and their levels.

Serial no	Input factor	Units	Levels				
			-2	-1	0	+1	+2
1	Peak current	Amperes	6	6.5	7	7.5	8
2	Back current	Amperes	3	3.5	4	4.5	5
3	Pulse rate	Pulses/second	20	30	40	50	60
4	Pulse width	%	30	40	50	60	70

Table 3. Welding conditions.

Power source	Secheron micro plasma arc machine (Model: PLASMAFIX 50E)
Polarity	DCEN
Mode of operation	Pulse mode
Electrode	2% thoriated tungsten electrode
Electrode diameter	1 mm
Plasma gas	Argon & hydrogen
Plasma gas flow rate	6 Lpm
Shielding gas	Argon
Shielding gas flow rate	0.4 Lpm
Purging gas	Argon
Purging gas flow rate	0.4 Lpm
Copper nozzle diameter	1 mm
Nozzle to plate distance	1 mm
Welding speed	260 mm/min
Torch position	Vertical
Operation type	Automatic

The method of designing such matrix is dealt elsewhere [19,20]. For the convenience of recording and processing the experimental data, the upper and lower levels of the factors are coded as +2 and -2, respectively and the coded values of any intermediate levels can be calculated by using the expression [21].

$$X_i = 2 \left[\frac{2X - (X_{\max} + X_{\min})}{(X_{\max} - X_{\min})} \right] \quad (1)$$

where X_i is the required coded value of a parameter X . The X is any value of the parameter from X_{\min} to X_{\max} , where X_{\min} is the lower limit of the parameter and X_{\max} is the upper limit of the parameter.

Table 4. Design matrix and experimental results.

Serial no	Peak current (amperes)	Back current (amperes)	Pulse rate (pulses/second)	Pulse width (%)	Grain size (microns)	Hardness (VHN)
1	-1	-1	-1	-1	20.812	198
2	1	-1	-1	-1	30.226	190
3	-1	1	-1	-1	21.508	199
4	1	1	-1	-1	27.536	193
5	-1	-1	1	-1	27.323	193
6	1	-1	1	-1	25.206	195
7	-1	1	1	-1	25.994	195
8	1	1	1	-1	23.491	197
9	-1	-1	-1	1	26.290	194
10	1	-1	-1	1	29.835	190
11	-1	1	-1	1	20.605	200
12	1	1	-1	1	27.764	193
13	-1	-1	1	1	30.095	190
14	1	-1	1	1	26.109	194
15	-1	1	1	1	27.385	193
16	1	1	1	1	25.013	195
17	-2	0	0	0	20.788	196
18	2	0	0	0	25.830	195
19	0	-2	0	0	31.663	188
20	0	2	0	0	27.263	193
21	0	0	-2	0	25.270	195
22	0	0	2	0	26.030	194
23	0	0	0	-2	24.626	195
24	0	0	0	2	26.626	194
25	0	0	0	0	24.845	196
26	0	0	0	0	24.845	196
27	0	0	0	0	20.145	200
28	0	0	0	0	24.845	195
29	0	0	0	0	20.045	201
30	0	0	0	0	24.845	195
31	0	0	0	0	20.445	198

3. Recording the Responses

3.1. Measurement of Grain Size

Three metallurgical samples are cut from each joint, with the first sample being located at 25 mm behind the trailing edge of the crater at the end of the weld and mounted using Bakelite. Sample preparation and mounting is done as per ASTM E3-1 standard. The samples are surface grounded using 120 grit size belt with the help of belt grinder, polished using grade 1/0 (245 mesh size), grade 2/0 (425 mesh size) and grade 3/0 (515 mesh size) sand paper. The specimens are further polished by using aluminum oxide initially and the by utilizing diamond paste and velvet cloth in a polishing machine. The polished specimens are etched by using 10% Oxalic acid solution to reveal the microstructure as per ASTM E407. Micrographs are taken using metallurgical microscope (Make: Carl Zeiss, Model: Axiovert 40MAT) at 100× magnifica-

tion. The micrographs of parent metal zone and weld fusion zone are shown in **Figures 1** and **2**.

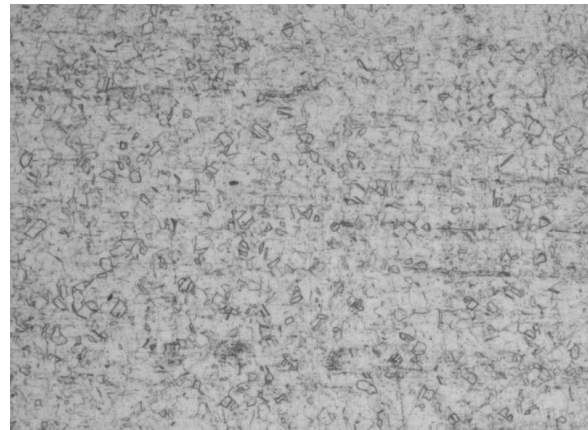


Figure 1. Microstructure of parent metal zone.

Grain size of parent metal and weld joint is measured by using Scanning Electron Microscope (Make: INCA Penta FETx3, Model: 7573). **Figures 3** and **4** indicate the measurement of grain size for parent metal zone and weld fusion zone. Average values of grain size are presented in **Table 4**.

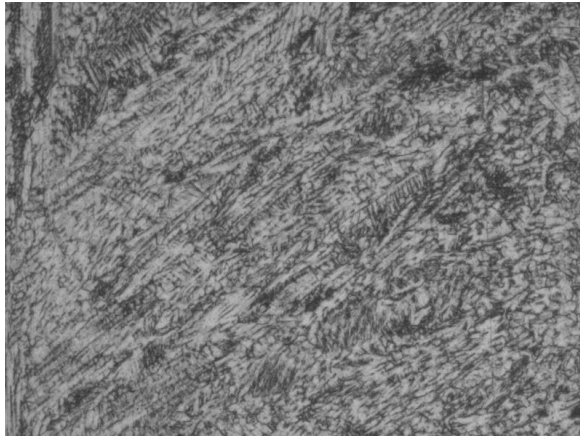


Figure 2. Microstructure of weld fusion zone.

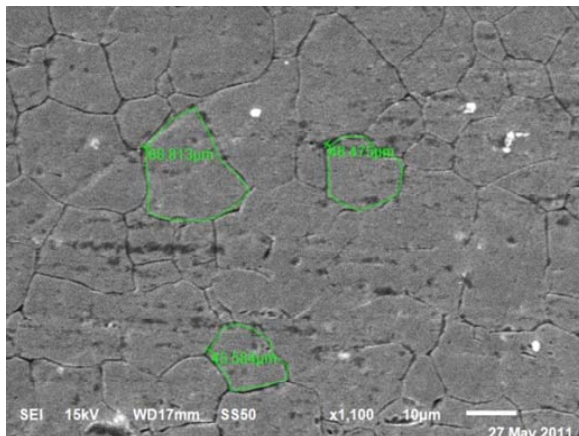


Figure 3. Grain size of parent metal.

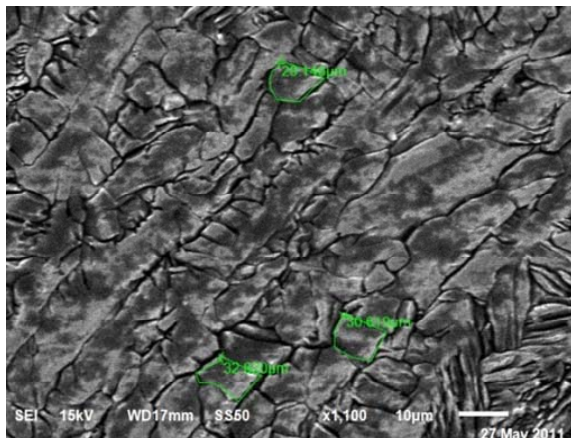


Figure 4. Grain size of weld fusion zone.

The grain size at the weld fusion zone is smaller than parent metal zone, which indicates sound weld joint.

3.2. Measurement of Hardness

Vickers's micro hardness testing machine (Make: MET-SUZAWA CO. LTD., JAPAN, Model: MMT-X7) was used to measure the hardness at the weld fusion zone by applying a load of 0.5 Kg as per ASTM E384. Average values of three samples of each test case are presented in **Table 4**.

4. Developing Mathematical Models

The grain size and hardness of the weld joint is a function of peak current (A), back current (B), pulse (C) and pulse width (D). It can be expressed as [22-24].

$$\text{Grain size } (G) \quad G = f(A, B, C, D) \quad (2)$$

$$\text{Hardness } (H) \quad H = f(A, B, C, D) \quad (3)$$

The second order polynomial equation used to represent the response surface "Y" is given by [19]:

$$Y = b_0 + \sum b_i x_i + \sum \beta_{ii} x_i^2 + \sum \sum b_{ij} x_i x_j + \epsilon \quad (4)$$

Using MINITAB 14 statistical software package, the significant coefficients were determined and final models are developed using significant coefficients to estimate grain size and hardness values of weld joint.

The final mathematical models are given by
Grain Size (G)

$$G = 22.859 + 1.052X_1 - 1.058X_2 + 0.315X_3 + 0.625X_4 + 1.640X_2^2 - 2.320X_1X_3 \quad (5)$$

Hardness (H)

$$H = 197.286 - 0.708X_1 + 1.292X_2 - 0.292X_3 - 0.542X_4 - 1.603X_2^2 + 2.188X_1X_3 \quad (6)$$

where X_1 , X_2 , X_3 and X_4 are the coded values of peak current, back current, pulse rate and pulse width respectively.

5. Checking the Adequacy of the Developed Models

The adequacy of the developed models was tested using the ANOVA technique. As per this technique, if the calculated value of the F_{ratio} of the developed model is less than the standard F_{ratio} (from F-table) value at a desired level of confidence (say 99%), then the model is said to be adequate within the confidence limit. ANOVA test results are presented in **Table 5** for all the models. From the table it is understood that the developed mathematical models are found to be adequate at 99% confidence level. The value of co-efficient of determination " R^{2*} " for the above developed models is found to be about 0.85.

Table 5. ANOVA test results for grain size and hardness.

Grain Size						
Source	DF	Seq SS	Adj SS	Adj MS	F	P
Regression	14	249.023	249.023	17.7873	6.10	0.000
Linear	4	65.207	65.207	16.3018	5.59	0.005
Square	4	91.443	91.443	22.8608	7.84	0.001
Interaction	6	92.372	92.372	15.3954	5.28	0.004
Residual error	16	46.639	46.639	2.9149		
Lack-of-fit	10	9.750	9.750	0.9750	0.16	0.994
Pure error	6	36.889	36.889	6.1481		
Total	30	295.661				
Hardness						
Source	DF	Seq SS	Adj SS	Adj MS	F	P
Regression	14	228.18	228.18	16.299	5.67	0.001
Linear	4	61.17	61.17	15.292	5.32	0.006
Square	4	83.64	83.64	20.910	7.27	0.002
Interaction	6	83.38	83.38	13.896	4.83	0.005
Residual error	16	46.01	46.01	2.876		
Lack-of-Fit	10	10.58	10.58	1.058	0.18	0.991
Pure Error	6	35.43	35.43	5.905		
Total	30	274.19				

Where DF = degrees of freedom; SS = sum of squares; MS = mean squares; F = fishers ratio.

6. Optimizing Using Hooke & Jeeves Method

Hooke and Jeeves algorithm [25] is used to search the optimum values of the process variables. In this paper the algorithm is developed to optimize the pulsed current MPAW process variables. The objective is to minimize grain size & maximize hardness. The coding for the Hooke Jeeves algorithm is written in MATLAB software.

The Hooke and Jeeves algorithm incorporates the past history of a sequence of iterations into the generation of a new search direction. It combines exploratory moves with pattern moves. The exploratory moves examine the local behavior of the function & seek to locate the direction of any stepping valleys that might be present. The pattern moves utilize the information generated in the exploration to step rapidly along the valleys.

Exploratory Move:

Given a specified step size which may be different for each coordinate direction and change during search. The

exploration proceeds from an initial point by the specified step size in each coordinate direction. If the function value does not increased the step is considered successful. Otherwise the step is retracted and replaced by a step in the opposite direction which in turn is retained in depending upon whether it success or fails. When all N coordinates have been investigated, the exploration move is completed. The resulting point is termed a base point.

Pattern Move:

A pattern move consists of a single step from the present base point along the line from the previous to the current base point.

A new pattern point is calculated as:

$$x_p^{(k+1)} = x^{(k)} + (x^{(k)} - x^{(k-1)})$$

where, $x_p^{(k+1)}$ is temporary base point for a new exploratory move.

If the result of this exploration move is a better point

then the previous base point $x^{(k)}$ then this is accepted as the new base point $x^{(k+1)}$. If the exploratory move does not produce improvement, the pattern move is discarded and the search returns to $x^{(k)}$, where an exploratory search is undertaken to find a new pattern.

Steps:

Step 1: Starting point $x^{(0)}$.

The increments Δ_i for $i = 1, 2, 3, \dots, N$.

Step reduction factor $\alpha > 1$.

A termination parameter $\varepsilon > 0$.

Step 2: Perform exploratory search.

Step 3: Was exploratory search successful (*i.e.* was a lower point found).

If yes go to Step 5.

Else continue.

Step 4: Check for the termination $\|\Delta\| < \varepsilon$ current pint approximation x_0 .

$\Delta_i = \Delta_i/\alpha$ for $i = 1, 2, 3, \dots, N$.

Go to Step 2.

Step 5: Perform pattern move

$$x_p^{(k+1)} = x^{(k)} + (x^{(k)} - x^{(k-1)})$$

Step 6: Perform exploratory research using $x_p^{(k+1)}$ as the base point; let the result be $x^{(k+1)}$.

Step 7: This step decides whether you are doing this operation for minimization or maximization.

a) If you applied the condition “Is $f(x^{(k+1)}) < f(x^{(k)})$?” then it is to find the maximum hardness.

b) If “Is $f(x^{(k+1)}) < f(x^{(k)})$?” then it is to find minimum grain size.

Step a) & b) results either Yes or No basing on the requirement of minimum grain size or maximum tensile strength. After getting the result continue with the following process.

If Yes set $x^{(k-1)} = x^{(k)}$.

$x^{(k)} = x^{(k+1)}$ go to Step 5.

Else go to Step 4.

From Tables 6 and 7 it is understood that the values predicted by Hooke and Jeeves algorithm and experimental values are very close to each other.

Table 6. Optimized pulsed current MPAW parameters for grain size.

	Hooke & Jeeves	Experimental
Peak current (amperes)	7.1299	7
Back current (amperes)	4.1299	4
Pulse rate (pulses/second)	42.5981	40
Pulse width (%)	52.5981	50
Grain size (microns)	21.1640	20.045

Table 7. Optimized pulsed current MPAW parameters for hardness.

	Hooke & Jeeves	Experimental
Peak current (amperes)	7.1127	7
Back current (amperes)	4.1127	4
Pulse rate (pulses/second)	42.2539	40
Pulse width (%)	52.2539	50
Hardness (VHN)	220.5633	201

7. Conclusion

Empirical relations are developed to predict grain size and hardness of pulsed current micro plasma arc welded AISI 304 L using Response Surface Method. The developed model can be effectively used to predict grain size and hardness values of pulsed current micro plasma arc welded joints. From the experiments conducted the minimum grain size of 20.045 microns and maximum hardness of 201 VHN are obtained for the input parameter combination of peak current of 7 Amperes, back current of 4 Amperes, pulse rate of 40 pulses/second and pulse width of 50%. From Hooke and Jeeves algorithm the minimum value of grain size obtained is 21.1640 microns for the input parameter combination of peak current of 7.1299 Amperes, back current of 4.1299 Amperes, pulse rate of 42.5981 pulses/second and pulse width of 52.5981%. Whereas maximum hardness obtained is 220.5633 VHN for the input parameter combination of peak current of 7.1127 Amperes, back current of 4.1127 Amperes, pulse rate of 42.2539 pulses/second and pulse width of 52.2539%. The values of grain size and hardness obtained experimentally and predicted using Hooke & Jeeves algorithm are within the limit.

8. Acknowledgements

The authors would like to thank Shri. R. Gopla Krishnan, Director, M/s Metallic Bellows (I) Pvt Ltd., Chennai, India for his support to carry out experimentation work.

REFERENCES

- [1] M. Balasubramanian, V. Jayabalan and V. Balasubramanian, “Effect of Process Parameters of Pulsed Current Tungsten Inert Gas Welding on Weld Pool Geometry of Titanium Welds,” *Acta Metallurgica Sinica (English Letters)*, Vol. 23, No. 4, 2010, pp. 312-320.
- [2] B. Balasubramanian, V. Jayabalan and V. Balasubramanian, “Optimizing the Pulsed Current Gas Tungsten Arc Welding Parameters,” *Journal of Materials Science and Technology*, Vol. 22, No. 6, 2006, pp. 821-825.
- [3] R. G. Madusudhana, A. A. Gokhale and R. K. Prasad,

- “Weld Microstructure Refinement in a 1441 Grade Aluminium-Lithium Alloy,” *Journal of Material Science*, Vol. 32, No. 5, 1997, pp. 4117-4126. [doi:10.1023/A:1018662126268](https://doi.org/10.1023/A:1018662126268)
- [4] D. K. Zhang and J. T. Niu, “Application of Artificial Neural Network Modeling to Plasma Arc Welding of Aluminum Alloys,” *Journal of Advanced Metallurgical Sciences*, Vol. 13, No. 1, 2000, pp. 194-200.
- [5] S.-C. Chi and L.-C. Hsu, “A Fuzzy Radial Basis Function Neural Network for Predicting Multiple Quality Characteristics of Plasma Arc Welding,” *9th IFSA World Congress and 20th NAFIPS International Conference*, Vol. 5, 2001, pp. 2807-2812.
- [6] Y. F. Hsiao, Y. S. Tarn and W. J. Huang, “Optimization of Plasma Arc Welding Parameters by Using the Taguchi Method with the Grey Relational Analysis,” *Journal of Materials and Manufacturing Processes*, Vol. 23, No. 1, 2008, pp. 51-58. [doi:10.1080/10426910701524527](https://doi.org/10.1080/10426910701524527)
- [7] K. Siva, N. Muragan and R. Logesh, “Optimization of Weld Bead Geometry in Plasma Transferred Arc Hardfacing Austenitic Stainless Steel Plates Using Genetic Algorithm,” *International Journal of Advanced Manufacturing Technology*, Vol. 41, No. 1-2, 2008, pp. 24-30. [doi:10.1007/s00170-008-1451-3](https://doi.org/10.1007/s00170-008-1451-3)
- [8] A. K. Lakshminarayana, V. Balasubramanian, R. Varahamoorthy and S. Babu, “Predicted the Dilution of Plasma Transferred Arc Hardfacing of Stellite on Carbon Steel Using Response Surface Methodology,” *Metals and Materials International*, Vol. 14, No. 6, 2008, pp. 779-789. [doi:10.3365/met.mat.2008.12.779](https://doi.org/10.3365/met.mat.2008.12.779)
- [9] V. Balasubramanian, A. K. Lakshminarayanan, R. Varahamoorthy and S. Babu, “Application of Response Surface Methodology to Prediction of Dilution in Plasma Transferred Arc Hardfacing of Stainless Steel on Carbon Steel,” *Science Direct*, Vol. 16, No. 1, 2009, pp. 44-53.
- [10] E. Taban, A. Dhooge and E. Kaluc, “Plasma Arc Welding of Modified 12% Cr Stainless Steel,” *Materials and Manufacturing Processes*, Vol. 24, 2009, pp. 649-656.
- [11] N. Kahraman, M. Taskin, B. Gulenc and A. Durgutlu, “An Investigation into the Effect of Welding Current on the Plasma Arc Welding of Pure Titanium,” *Kovove Mater*, Vol. 48, 2010, pp. 179-184.
- [12] N. Srimath and N. Muragan, “Prediction and Optimization of Weld Bead Geometry of Plasma Transferred Arc Hardfacing Valve Seat Rings,” *European Journal of Scientific Research*, Vol. 51, No. 2, 2011, pp. 285-298.
- [13] K. S. Prasad, C. S. Rao and D. N. Rao, “Prediction of Weld Quality in Plasma Arc Welding Using Statistical Approach,” *International Journal of Science and Technology in Production and Manufacturing Engineering*, Vol. 3, No. 4, 2010, pp. 1-7.
- [14] K. S. Prasad, Ch. S. Rao and D. N. Rao, “Optimizing Pulsed Current Micro Plasma Arc Welding Parameters to Maximize Ultimate Tensile Strength of Inconel 625 Nickel Alloy Using Response Surface Method,” *International Journal of Engineering, Science and Technology*, Vol. 3, No. 6, 2011, pp. 226-236.
- [15] K. S. Prasad, Ch. S. Rao and D. N. Rao, “Prediction of Weld Pool Geometry in Pulsed Current Micro Plasma Arc Welding of SS304L Stainless Steel Sheets,” *International Transaction Journal of Engineering, Management & Applied Sciences & Technologies*, Vol. 2, No. 3, 2011, pp. 325-336.
- [16] K. S. Prasad, Ch. S. Rao and D. N. Rao, “A Study on Weld Quality Characteristics of Pulsed Current Micro Plasma Arc Welding of SS304L Sheets,” *International Transaction Journal of Engineering, Management & Applied Sciences & Technologies*, Vol. 2, No. 4, 2011, pp. 437-446.
- [17] K. S. Prasad, Ch. S. Rao and D. N. Rao, “Prediction of Weld Bead Geometry in Plasma Arc Welding Using Factorial Design Approach,” *Journal of Minerals & Materials Characterization & Engineering*, Vol. 10, No. 10, 2011, pp. 875-886.
- [18] K. S. Prasad, Ch. S. Rao and D. N. Rao, “Establishing Empirical Relationships to Predict Grain Size and Hardness of Pulsed Current Micro plasma Arc Welded Inconel 625 Sheets,” *Journal of Materials & Metallurgical Engineering*, Vol. 1, No. 3, 2011, pp. 1-10.
- [19] D. C. Montgomery, “Design and Analysis of Experiments,” 3rd Edition, John Wiley & Sons, New York, 1991, pp. 291-295.
- [20] G. E. P. Box, W. H. Hunter and J. S. Hunter, “Statistics for Experiments,” John Wiley & Sons, New York, 1978, pp. 112-115.
- [21] S. Babu, T. S. Kumar and V. Balasubramanian, “Optimizing Pulsed Current Gas Tungsten Arc Welding Parameters of AA6061 Aluminium Alloy Using Hooke and Jeeves Algorithm,” *Transactions of Nonferrous Metals Society of China*, Vol. 18, No. 5, 2008, pp. 1028-1036. [doi:10.1016/S1003-6326\(08\)60176-4](https://doi.org/10.1016/S1003-6326(08)60176-4)
- [22] W. G. Cochran and G. M. Cox, “Experimental Designs,” John Wiley & Sons Inc., London, 1957.
- [23] T. B. Barker, “Quality by Experimental Design,” ASQC Quality Press, Marcel Dekker, 1985.
- [24] W. P. Gardiner and G. Gettinby, “Experimental Design Techniques in Statistical Practice,” Horwood, Chichester, 1998.
- [25] D. Kalyanmoy, “Optimization for Engineering Design,” Prentice Hall, New Delhi, 1988.